An Experimental Model for Determination of the Entrainment in Column Flotation Based on Operation Parameters

Reza Zolfaghari and Mohammad Karamoozian*

Faculty of Mining, Petroleum & Geophysics Engineering, Shahrood University of Technology, Shahrood, Iran

Article Info	Abstract
	In flotation, entrainment (ENT) affects the recovery of the concentrate, and the entrainment model is often supposed to be only a function of particle size in models. Some research shows that other variables may also significantly affect ENT. In this study, some flotation experiments executed using a mixture of pure quartz as the valuable mineral and a pure magnetite sample as the gangue mineral to investigate the effects of other variables, such as solid content, airflow rate, frother, and collector dosages, on ENT. The results showed ENT varied from 0.071 to 0.851 is different, while the entrainment recovery was between 0.006 to 0.23, which means that the difference is statistically significant. ENT affected by (1) collector dosage, (2) frother dosage, (3) solid content, (4) the interaction between airflow rate and solid content and, (5) the interaction between airflow rate and frother dosage. An empirical statistical model is presented based on operational parameters. As the present models for ENT incorporate just particle size, it is not enough to predict gangue recovery in industrial applications by keeping the operating conditions constant. This novel model can predict ENT based on different operational parameters. The developed model is presented based on the particle mass by changing the operation parameters.

1. Introduction

Flotation is the most effective method in mineral processing, serving as a primary operational unit in most processing plants. It is the most common method used to separate valuable minerals [1]. Flotation method is used for almost all industrial minerals and coal and sulfide minerals [2, 3]. The industrial use of column cells began in 1980, but extensive research on them was conducted by Pierre Boutin and Rémi Tremblay in 1962. Their work related to the initial laboratory research on solvent extraction at Eldorado Mine [4]. The first successful application of mixed cell column related to a Canadian column flotation for washing molybdenum in Mines Gaspe Noranda Les in 1981[5]. Today, column flotation is considered an acceptable technology in many applications, especially for the final enrichment of metal sulfides (copper, zinc, lead, and molybdenite) and the flotation of phosphate ores and coal [6]. Most of the copper producers in the

world use flotation as the final step of cleaner [7]. Flotation was strongly influenced by changes in input pulp characteristics, device operating parameters, chemical consumption, pH, etc. [8-10]. The advantages of flotation can be mentioned as reducing operation time, reducing energy consumption, and being more selective, which have been studied by many researchers [11-14]. The results showed that the froth was the key to understanding the general performance of the process, and the characteristics of the froth can be used as an effective indicator of the performance status of the process. In many flotation units, operational variables, such as chemical reagents, airflow rate, and pulp surface, are performed through observations and adjusted with the froth characteristics [15-17]. However, there are many difficulties in controlling the flotation operation by visual inspection. ENT was generally considered a 2 step: step one, mineral particles ascend from the

✉ Corresponding author: m.karamoozian@shahroodut.ac.ir (M. Karamoozian).

bottom region below the pulp/froth interface to the froth phase, and step two, tracer particles are transferred from the froth to the concentrate. These two phases highly depend on the processes occurring in both the pulp and froth phases. [18].

Consequently, the Recovery by ENT connected to the situation of dispersion of solids in the pulp, drainage in the froth phase, and water recovery. A classification function was proposed to describe the drainage in the froth [10].

$$CF_i^f = \frac{(mass\ of\ free\ gangue\ per\ unit\ mass\ of\ water)\ concentrate}{(mass\ of\ free\ gangue\ per\ unit\ mass\ of\ water)\ top\ of\ pulp} \tag{1}$$

Where CF_i^f represents the drainage in the froth phase, the subscript i indicates the particle size and the superscript f indicates the froth phase.

$$CF_i^p = \frac{(mass\ of\ free\ gangue\ per\ unit\ mass\ of\ water)pulp}{(mass\ of\ free\ gangue\ per\ unit\ mass\ of\ water)tailing} \tag{2}$$

Where the superscript P is representing the pulp phase. The overall sorting effect can be determined by:

$$ENT_i = CP_i^P . CP_i^f \tag{3}$$

Where ENT_i is the degree of entrainment that represents the overall classification effect in pulp and froth (for particle size i). ENT_i can be directly used to estimate the Recovery of gangue by combining these two classification effects. The Recovery of gangue is practically achieved by water recovery modified by the ENT. There are 2 models of gangue recovery by the entrainment from past research (see Equations (4) and (5)) [19-21].

$$R_{ent,i} = \frac{ENT_i . R_w}{1 + R_w . (ENT_i - 1)} \tag{4}$$

$$R_{ent,i} = ENT_i . R_w \tag{5}$$

Where $R_{ent,i}$ is recovery by the entrainment, and R_w is water recovery. Thus, it can provide a very accurate amount of gangue recovery by the ENT. Equation (5) is the simplified form of Eq. (4), which could be used when R_w is less than 30% or for very fine particles regardless of R_w. This research has been conducted on ENT and the factors affecting it. In the froth phase, particle mass and operation conditions are always necessary in the ENT process [22-24].

In past research, ENT has been experimentally modeled based on particle size while keeping constant other operational parameters. In these studies, either only particle sizes and densities were varied, or one or two operational parameters were changed, with no consensus among researchers on the choice of parameters. [25-28]. It is better to model the ENT based on particle characteristics considering the operating conditions of the column flotation, which is the result of both the size and density of the particle (Quartz).

The experimental model presented by Savassi et al. (1998), illustrated below, has been widely used for predicting the ENT.

$$ENT_i = \frac{2}{\exp\left[2.292\left(\frac{d_i}{\xi}\right)^{adj}\right] + \exp\left[-2.292\left(\frac{d_i}{\xi}\right)^{adj}\right]} \tag{9}$$

$$adj = 1 - \frac{\ln\left(\frac{1}{\zeta}\right)}{\exp\left(\frac{d_i}{\zeta}\right)} \tag{10}$$

Various models have been developed using different parameters for ENT [31, 36–41]. Additionally, Zheng et al. presented models to estimate ENT [29]. Operational variables could significantly change the ENT. However, it was still unclear to what extent the ENT is affected by and interacts with other operational variables. Therefore, in this study, batch flotation experiments were conducted to identify the critical parameters of the ENT. The goal was to develop fundamental knowledge to enable the influence of operational parameters of the ENT in column flotation applications and also provide a model based on operational parameters.

ENT is an essential factor in the cleaner by using column flotation in its determination. The effect of operational variables should be considered (such as airflow rate, solid percentage, collector dosage, etc.). Previous studies had mainly discussed the theory and presentation of the model or only the effect of one operating variable. The

goal of this research was to investigate the developed model of the ENT based on mass particles in the column flotation with the effect of flotation operating variables. [1, 25-28]. The materials, reagents, and methods used are presented in the following sections.

2. Materials and Methods
2.1. Minerals and chemicals used

The flotation tests were performed in one step with a mineral substance. Quartz particles with purity above 97% were used (Table 1). Also, for flotation tests with quartz mineral, washing water was not used because high-purity quartz was used.

Table 1. Results of semi-quantitative XRD analysis of silica sample

Composition	LOI	SiO₂	Cr₂O₃	P₂O₅	K₂O	Na₂O	MgO	Al₂O₃	CaO	TiO₂	Fe₂O₃
Percent	0.01	97.05	0.48	0.17	0.33	0.06	0.12	0.53	0.43	0.11	0.71

The mineral was quartz ($S_G = 2.66$) and the gangue was magnetite ($S_G = 4.75$). This pure mineral material obtained from Hamadan Silica Company and Ehya Sepahan Ore Mine.

2.1.1. Reagents

Sodium hydroxide solution and Dodecylamine were prepared by EMD Millipore Corporation. Its chemical structure is shown in table 2. The frother agent was Methyl Iso Butyl Carbinol (MIBC), which was produced by Isfahan Co Polymer Chemical Company. All the reagents were prepared before the flotation experiments and the tap water of Mashhad was utilized (table 3).

2.2. Designing experiments and sample preparation

The response surface test design method (Anderson-Cook et al., 2009) with four independent variables has been used to design, examine the influence of operational variables on ENT. The independent variables used include (Figure 1): solid content (5, 10, and 15%), airflow rate (10, 20, and 30 mm/s), frother dosage (10, 20, and 30 g/t), and the collector dosage was (100 and 200 g/t). A prototype of quartz was combined with a prototype of the mineral gangue (magnetite), 17% by weight of quartz feed, and the total mineral along with gangue form approximately 5-15% by weight of solid materials in the flotation column. The preparation time was 60 and 30 seconds for the collector and froth, respectively. Aeration started when the mixture of quartz and magnetite was added to the flotation column. The depth of the froth was considered to be 7 cm from the edge of the launder. Experimental results were analyzed using DX 13 software.

Each independent variable studied on the ENT (table 4). Three center points replicate experiments used to calculate experimental error (test number was 8, 18, and 27). All runs performed under relatively homogeneous conditions.

Table 2. Chemicals and conditions used for quartz flotation.

Mineral	Collector	pH adjuster	Frother
Quartz	Dodecylamine	Sodium hydroxide	MIBC
SiO_2	$CH_3(CH_2)_{10}CH_2NH_2$	NaOH	$(CH_3)_2CHCH_2CH(OH)CH_3$

Table 3. The combination of Mashhad water (mg/L).

Na^+	K^+	Ca^{2+}	Mg^{2+}	Si^{4+}	Cl^-	SO_4^{2-}	CO_3^{2-}
54.65	1.16	28.2	27.5	1.04	96	12.3	21.5

Table 4. Independent variables in the CCD method with five levels and three repetitions at the central point

Parameter	Symbol	Unit	Levels of independent parameters				
			(Alpha 2-)	-1	·	+1	(Alpha 2+)
Solid content	A	%	0	5	10	15	20
Frother dosage	B	g/t	0	10	20	30	40
Air flow rate	C	L/min	2.5	4.5	6.5	8.5	10.5
Collector dosage	D	g/t	50	100	150	200	250
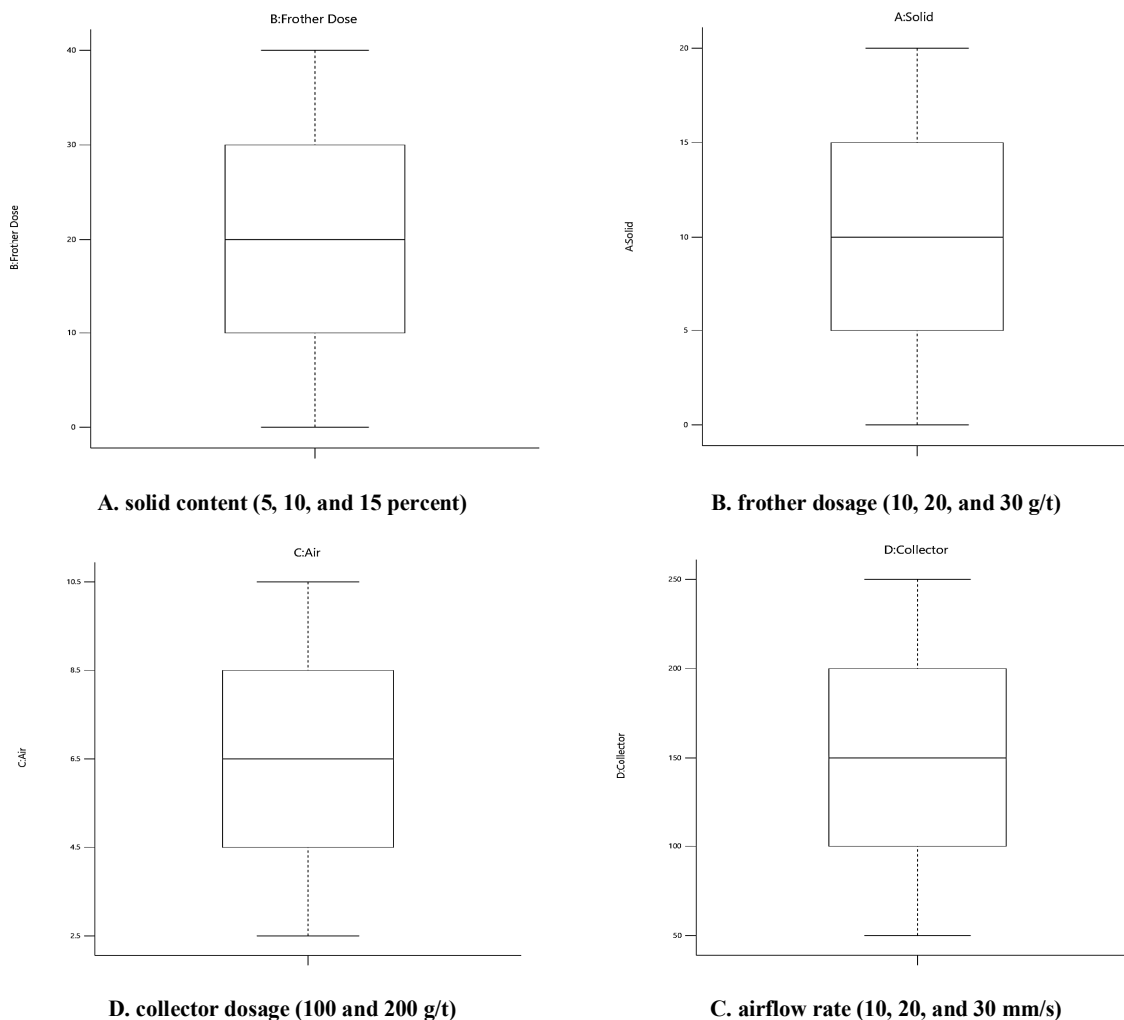
Figure 1. Operating variables in the experiments.

A. solid content (5, 10, and 15 percent)

B. frother dosage (10, 20, and 30 g/t)

D. collector dosage (100 and 200 g/t)

C. airflow rate (10, 20, and 30 mm/s)

2.3. Test method and flotation device

The first step was to screen the quartz in the size class of +74-149 (μm) because it is the closest size to tracing particles, the size distribution of both quartz and magnetite is provided in figure 2-A, B, respectively. Then the sample(s) were fed into a transparent column flotation with a fixed lip to the inner diameter 11 cm and height of 100 cm (Figure 3).
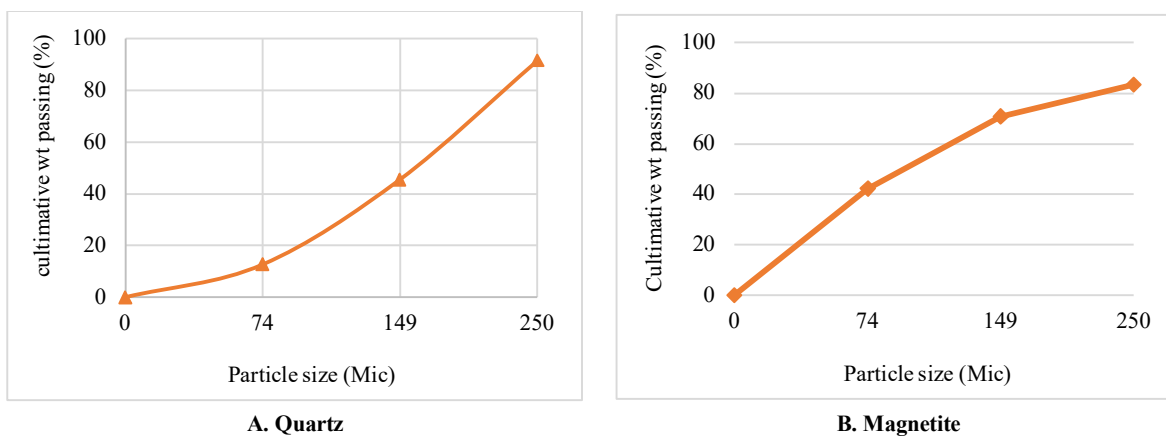

A. Quartz

B. Magnetite

Figure 2. The size distribution of Quartz and Magnetite.

The froth height does not change without changing the practical pulp volume. The production of the tests was collected within 7 minutes. The froth was scratched every 5 seconds. The froth scratcher is designed so that only the top froth of the launder edge of the column was removed to minimize any disturbance to the structure of the bottom froth. Tap water periodically was added to the experiment to maintain the pulp level by using a peristaltic pump.
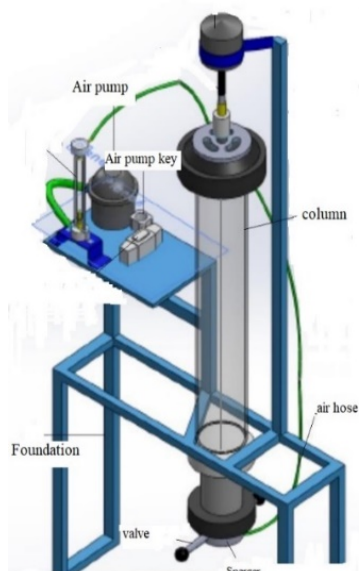
2.4. Calculation of the Recovery of entrainment, R_w, and the ENT

The gangue mineral (magnetite) liberated entirely and must be hydrophilic in the presence of the Dodecylamine collector, it could be recovered by ENT in the concentrate.

Figure 3. Schematic of column flotation device [33].

$$\text{ENT}_i = \frac{(\text{mass of free gangue per unit mass of water})_{\text{concentrate}}}{(\text{mass of free gangue per unit mass of water})_{\text{tail}}} \qquad (6)$$

In this research, ENT was calculated assuming the amount of waste in the column at the end of the test.

In past research, R_w was computed using 2 ways: The proportion of water in the column was recovered to the launder, or the flowrate of water to the concentrate [33]. In this study, the 1st method was used.

3. Results and discussion
3.1. Flotation results

The experimental results are shown in Table 5. The gangue used in these experiments was utterly free, and it could probably be supposed that they were recovered only through entrainment to the concentrate. Therefore, the change in the amount of the entrainment is caused by the changes in the operating parameters.

ENT in different experiments was a vital function of concentrate recovery, which varies between experiments (see Figure 4). In other words, entrainment is affected by the mass recovery of material.
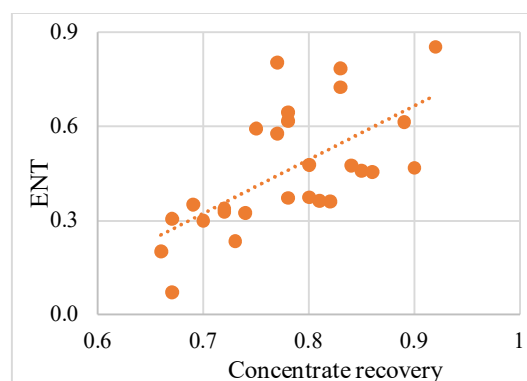

Figure 4. Plot of entrainment recovery versus concentrate recovery

Table 5. Experiments designed by the central composite method to investigate dependent variables.

Test number	Independent variables				Dependent variables			
	Solid content	Frother Dosage	Air flow rate	Collector dosage	R_w	Con Rec	ENT	$R_{ent\,i}$
	%	g//ton	L/min	g/ton		%		
1	15	10	8.5	200	0.24	82	0.35	0.102
2	10	40	6.5	150	0.21	83	0.72	0.161
3	20	20	6.5	150	0.16	90	0.46	0.082
4	10	0	6.5	150	0.15	70	0.29	0.050
5	5	10	8.5	200	0.19	69	0.35	0.076
6	10	20	6.5	50	0.27	72	0.33	0.111
7	15	30	8.5	200	0.22	89	0.61	0.147
8	10	20	6.5	150	0.17	78	0.61	0.112
9	15	30	8.5	100	0.22	86	0.45	0.113
10	15	30	4.5	100	0.2	85	0.45	0.103
11	5	30	4.5	200	0.15	77	0.80	0.124
12	15	10	4.5	200	0.16	84	0.47	0.083
13	5	10	8.5	100	0.16	67	0.30	0.055
14	10	20	10.5	150	0.25	78	0.37	0.110
15	15	10	8.5	100	0.23	80	0.47	0.125
16	5	30	8.5	100	0.23	74	0.32	0.088
17	5	10	4.5	100	0.08	67	0.07	0.006
18	10	20	6.5	150	0.18	75	0.59	0.115
19	5	30	4.5	100	0.14	73	0.23	0.037
20	15	30	4.5	200	0.15	92	0.85	0.131
21	10	20	6.5	250	0.28	83	0.78	0.233
22	0	20	6.5	150	0.07	66	0.20	0.015
23	5	10	4.5	200	0.08	72	0.32	0.028
24	5	30	8.5	200	0.25	78	0.64	0.177
25	15	10	4.5	100	0.19	81	0.36	0.078
26	10	20	2.5	150	0.1	80	0.37	0.040
27	10	20	6.5	150	0.15	77	0.57	0.092

ENT values were calculated using equation (6). The ENT ranged from 0.071 to 0.851, meaning ENT changes significantly in different situations. The Recovery of the concentrate was high in all experiments (66-92%). The Recovery increased, but the selectivity decreased. Increasing of collector and frother dosage changed the froth structure in column flotation.

However, above a certain collector and frother concentration value, effervescence conditions destroyed and turbulence flow conditions formed producing large froth. In the previous work [42], this issue was suppressed by using a horizontal baffle. Therefore, collector and frother dosage was one of the significant parameters in ENT. The effervescence situations which were favored in column flotation were lost and turned to the churn-turbulent flow parameters.

3.2. Statistical significance of operational parameters

The impacts and interactions of 4 factors on the ENT at the 95% confidence level were analyzed using DX 13. The results resumed in Table 6. ENT was significantly affected by the operating parameters (including solid content, frother dosage and collector dosage). In addition, the F value of

501.65 for the "fit" model in Table 7 also shows that there is only a 0.01% chance that an F value of this magnitude is due to noise. In this case, the factors A, B, C, D, AC, AD, BC, BD, CD, A², B² and C² are significant model terms. The F value of the disproportion of 0.23 shows that the disproportion is not substantial compared to the net error. There is a 95.57% chance that an F value of this magnitude is due to misfit due to noise.

The normal probability diagram of the residuals shows that the error terms are generally distributed throughout the entire study. The linear pattern of the results of this study shows a normal distribution (Figure 5).

Figure 6 shows the saturation. According to Figure 5, ENT was significantly affected by (1) the collector dosage, (2) the frother dosage and, (3) the solid content. This model introduced for certain material. In other word for copper, coal or zinc the priority of affecting factor and the precision of model may be different. The collector dosage has a significant impact on both steps of the ENT process. Increase in the collector dosage will increase in the R_w and suspended solids enter the froth phase from the top of the pulp region. Meanwhile, varying the dosage of the collector and frother changes the froth structure, as well as the retention time of froth and entrained particles in the

froth phase. This, in turn, affects the extent of drainage and the preferential drainage of particles of different sizes. However, the final outcome of ENT depends not only on particle entrained size but also on column operational parameters such as the froth structure and column parameters.
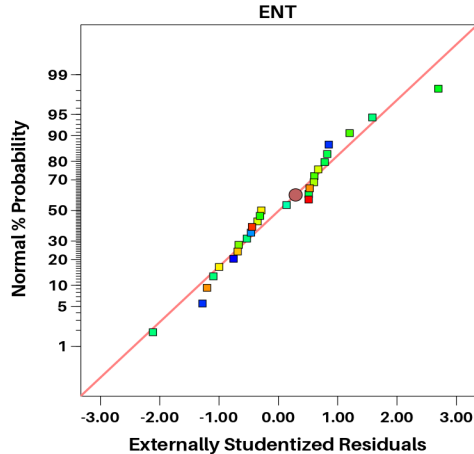
The quality evaluation indices of the ENT model in Table 8 shows the predicted R² of 0.9930 is in reasonable agreement with the adjusted R² of 0.99630. The ratio of the 90.59 model indicates a sufficient signal. This model can be used to move in the design space.

Figure 5. The standard scatter diagram of the results of the independent variables in the central composite design
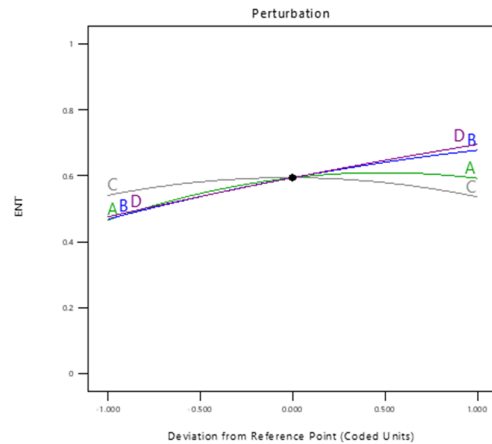
Figure 6. Saturation plot generated by DX 13 when analyzing the effect of experimental variables on the ENT model.

Table 6. The results of a statistical evaluation of the effect of operating parameters and their mutual impact on the ENT

Source	Sum of Squares	Df	Mean Square	F-value	p-value	Effect on response
Model	0.9693	13	0.0746	178.82	< 0.0001	significant
A-Solid	0.1405	1	0.1405	336.94	< 0.0001	
B-Frother Dosage	0.0041	1	0.0041	9.74	0.0081	
C-Air flow rate	0.1401	1	0.1401	336.09	< 0.0001	
D-Collector Dosage	0.0288	1	0.0288	68.96	< 0.0001	
AC	0.0114	1	0.0114	27.46	0.0002	
AD	0.0259	1	0.0259	62.09	< 0.0001	
BC	0.0203	1	0.0203	48.60	< 0.0001	
BD	0.0814	1	0.0814	195.15	< 0.0001	
CD	0.0534	1	0.0534	128.15	< 0.0001	
A²	0.0909	1	0.0909	217.93	< 0.0001	
B²	0.0095	1	0.0095	22.78	0.0004	
C²	0.0661	1	0.0661	158.60	< 0.0001	
Residual	0.0054	13	0.0004			
Lack of Fit	0.0046	11	0.0004	1.10	0.5700	not significant
Pure Error	0.0008	2	0.0004			
Cor Total	0.9747	26				
Model	0.9693	13	0.0746	178.82	< 0.0001	significant

Table 8. Quality evaluation indices of the ENT model

Fit Statistics			
Std. Dev.	0.0118	R²	0.9983
Mean	0.4605	Adjusted R²	0.9963
C.V. %	2.56	Predicted R²	0.9930
		Adeq Precision	90.5908

A mathematical model could be established between ENT and the factors (see equation 7).

Here, the levels must be specified in basic units for each factor.

$$ENT = -1.917 + 0.112\,A + 0.012\,B + 0.328\,C + 0.005\,D - 0.0003\,AB - 0.002\,AC - 0.0001\,AD$$
$$- 0.001\,BC + 0.0001\,CD \tag{7}$$

A is solid content, B is frother dosage, C is airflow rate, and D is collector dosage.

3.3. The effect of operational parameters
3.3.1. The effect of solid content

The solid percentage had an impact on the ENT. Figure 10 shows the ENT vs. solid content for all tests performed. The ENT changed from 7% in 5% solids to 85% in 15% solids (Figure 11).

The ENT increased with increasing pulp solids content, consistent with the past literature [27, 31]. As shown in Figure 7, increasing ENT (0.071-0.851) can result in a significant variation in concentrate recovery (66-92%), regardless of R_w, which indicates the effect of operation variables on the ENT was substantial and, it should not be ignored when modeling the ENT. Based on statistical analysis, the solid content and its interaction with other variables have the same

effect on ENT. This was the result of increasing the ENT and R_w [30, 31].

According to Figure 8, the increase in the size of tracer particles with increasing solid content was probably related to the reality that they tend to shift with water in the interface region due to the higher settling velocity. Since the amount of solid suspension in the pulp phase may be more substantial for the mineral with a higher solid content, and as a result, larger particle sizes were transferred from the pulp to the froth, it should not be neglected when modeling the ENT. In summary, the graph indicates a positive polynomial relationship between ENT and tracked particle size, with ENT explaining 77.51% of the variance in tracked particle size. This suggests a relatively strong correlation, though operational factors can also influence the tracked particle size.
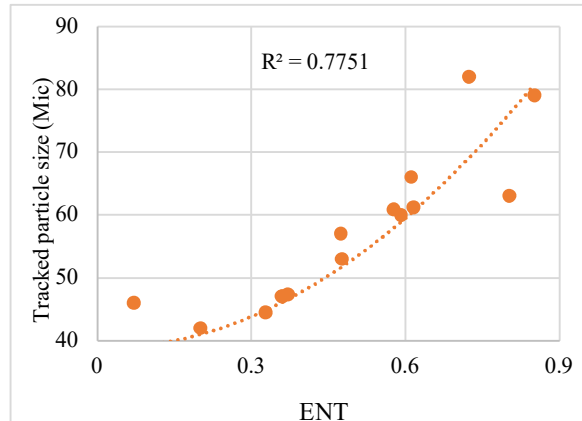
Figure 7. ENT as a function of solid content

Figure 8. Tracked particle size as a function of ENT

In Figure 9, the interaction between solid content and frother dosage is observed. In this interaction, the variables have direct and reciprocal effects, so their simultaneous increase and decrease could directly increase and decrease the amount of ENT, respectively. In other words, when both variables were at the lowest possible value, the amount of ENT was also minimized, and the opposite is also true. Also, in Figure 10, the variables act inversely to each other, assuming, for example, the increase of solid content from 5 to 15 (%). There is an upward trend in the response at low values of airflow rate, but with the continuous growth of airflow rate, this trend takes a downward trend.

In the interaction of solid content and collector dosage (Figure 10), with the increase of solid percentage and collector dosage, the value of ENT increases from 5-15 (%) and 100 to 200 (g/t), respectively, in solid =15(%) and collector =200 (g/t), the amount of ENT reaches the maximum. If the goal is to reduce the amount of ENT, the opposite of this process should be done; also, the mutual effect of these two variables is direct for each other, with the difference that collector dosage has a more significant impact on ENT value than solid content with increasing the solids content: the viscosity of pulp zone increases and harder move of bubbles may happen. Furthermore, the weak space behind the bubble is affected and the

entrainment increased (Figure 11). Minerals with low solid content have a higher chance of sinking and moving via plateau boundaries in the froth phase than minerals with higher solid content. Therefore, as the pulp solid content decreases, ENT decreases.
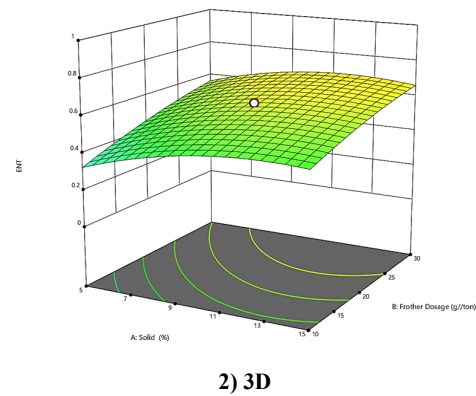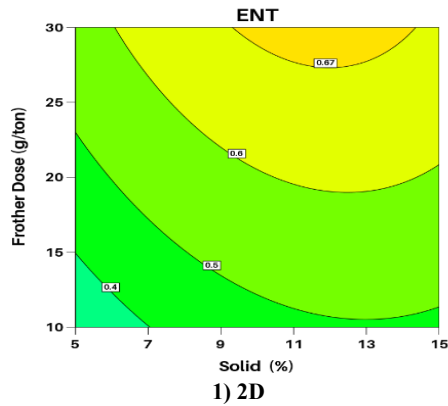

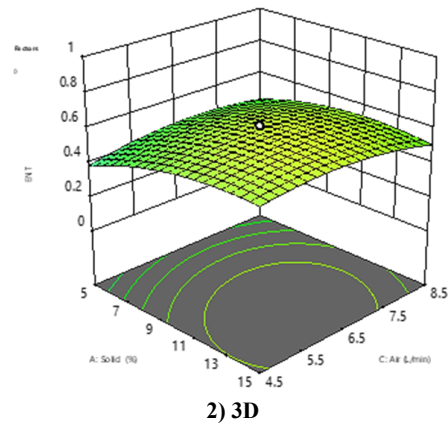**Figure 9. Solid content-frother dosage interaction diagram on ENT as 1) 2D and 2) 3D**
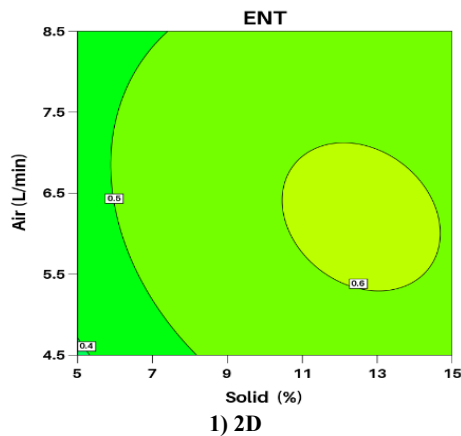

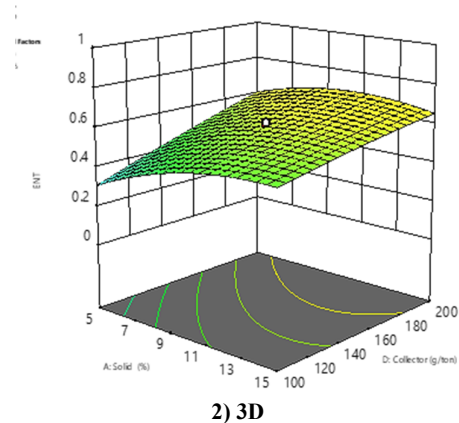**Figure 10. Solid content-airflow rate interaction diagram on ENT as 1) 2D and 2) 3D**
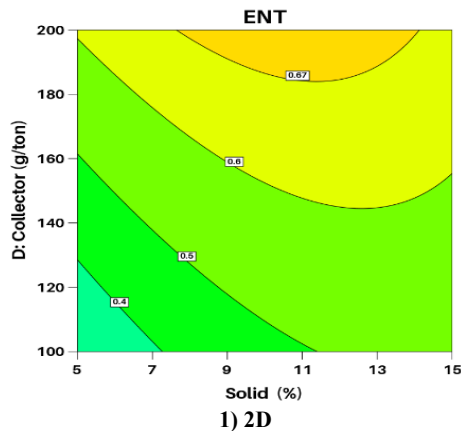

Figure 11. Solid content-collector dosage interaction diagram on ENT as 1) 2D and 2) 3D

3.3.2. The effect of frother dosage

Superficial airflow rates and frother dosage are all directly influential factors for each other. When airflow rate and the frother dosage increased, the ENT increased [42]. Variation in the ENT is caused by the frother dosage, a variable that affects the structure of the froth, including its stability and bubble size distribution. The frother agent can be discharged during the flotation test and transferred to the concentrate [27-33]. The flotation test was carried out using quartz in different concentrations

of MIBC. The test was performed 7 minutes, with airflow rate of 8.5 liters per minute and solid content of 15 percent. Figure 15 shows the change in the ENT when the frother dosage increased.
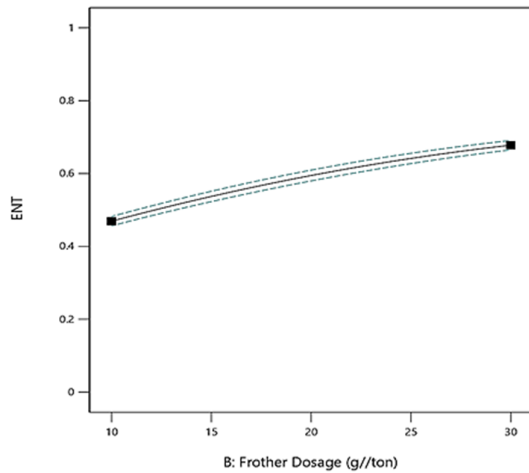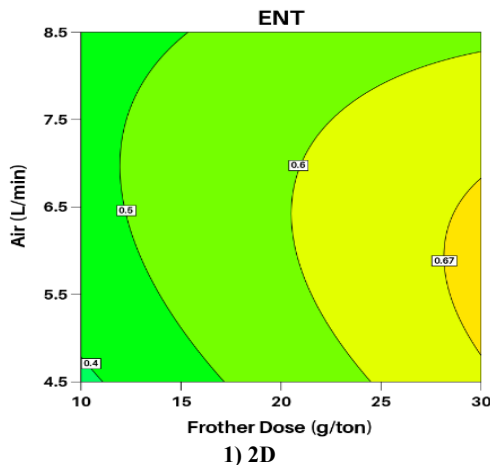

Figure 12. Effect of MIBC frother dosage factor on overall ENT.

Regarding ENT, changes in the frother dosage mainly affected the drainage process in the froth phase. Meanwhile, a change in the froth residence time can also result in a change in froth characteristics. As a result, ENT increased with an increase in the frother dosage figure 12. ENT_1 with

the concentration of MIBC reduced from 30 g/t to 10 g/t to obtain a comparable ENT level in surface response tests. A measured change in the ENT occurs (figure 12).

Based on the statistical analysis, the frother dosage and its interaction with other variables has a significant effect on ENT. The effect of frother dosage as a function of ENT was measured at different solid content. An increase in ENT was observed with increasing frother dosage, which was statistically significant and expected to lead to a substantial change in $R_{ent,i}$. There was an increase in gangue recovery with increasing frother dosage in the test results. The enhancement of gangue recovery by ENT is consistent with observations made in other studies in the literature [32-34]. The amount of frother dosages improves the R_w and ENT, thereby affecting the gangue recovery.

Analyzing the interaction of frother dosage and airflow rate is the opposite of solid content-collector dosage interaction (figure 13). In such a way that the increasing trend of the response is more significant in the X axis and, with the increase of frother agent and air flow rate, the value of ENT increases. Reducing the frother dosage creates a stable froth phase by allowing enough time for dewatering without excessive bubble cohesion.
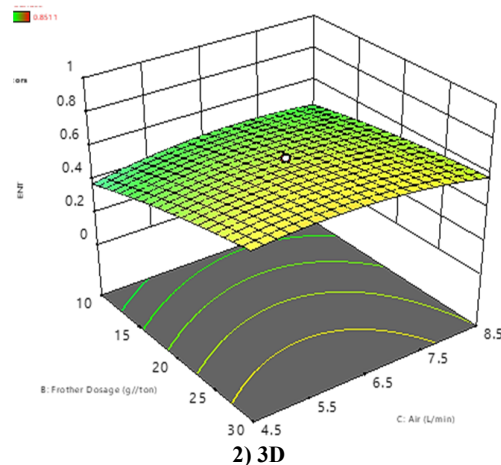

Figure 13. frother dosage-airflow rate interaction diagram on ENT as 1) 2D and 2) 3D

According to Figure 14, the mutual effects of the frother-collector dosage on ENT have a direct relationship. In this interaction, at the lowest possible amount of collector dosage, with the increase of frother agent from 10 to 30 (g/t), an upward trend of ENT is observed. This trend becomes much higher with the simultaneous increase of frother dosage, and at collector dosage

=200 (g/t) and frother dosage = 30 (g/t) the amount of ENT reaches the maximum.

Therefore, changes in gangue recovery due to the frother agent result from variations in both R_w mode and ENT. Changing the frother dosage altered the froth structure, which affected the movement rate of water and suspended particles.
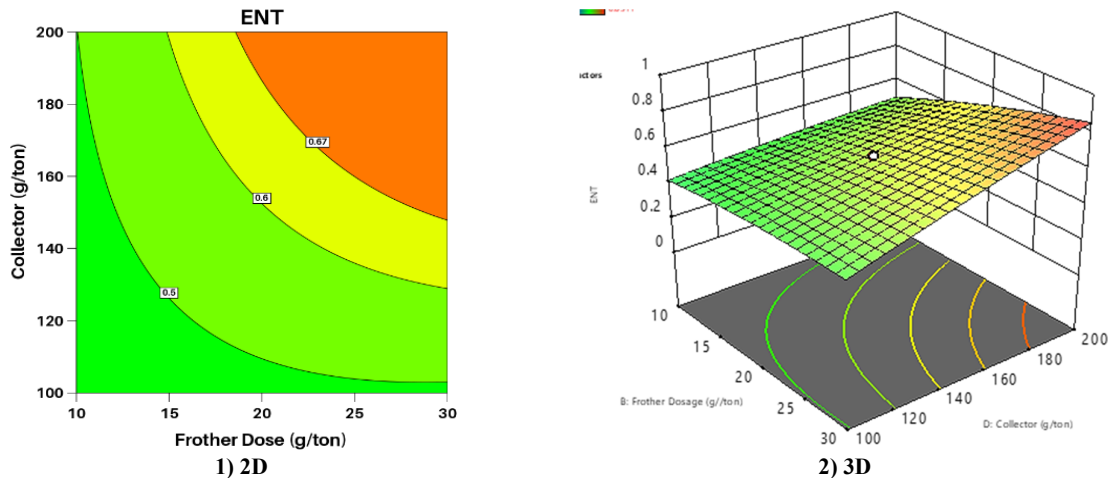
Figure 14. Diagram of the frother-collector dosage interaction on ENT as 1) 2D and 2) 3D

3.3.3. Effect of airflow rate

The airflow rate is one of the operational parameters that did not affect ENT. The interaction between airflow rate and frother agent and between airflow rate and solid content affected the ENT.

At a low airflow rate, the water content in the froth phase decreases rapidly with the increase in the height of the froth [5]. Low water content may lead to the narrowing of plateau boundaries, which causes resistance and, as a result, less discharge of solids [23]. At shorter froth profundity, this thinning may not happen, leading to a more significant amount of solids drainage and reducing ENT. At higher airflow rates, the "wetter froth" may not be thin enough at the plateau boundaries to prevent solid drainage. Suspended particles in the pulp phase may move more freely, reversing the observed trend. Now, there may be more time for drainage, and thus, ENT is reduced

3.3.4. Effect of collector dosage

The collector agent and its interaction with other variables affected ENT. Figure 15 shows the effect of the collector agent as a function of ENT measured at different unstained flotation concentrations at different collector dosages. The effect of collector dosage on ENT is shown in Figure 18. An increase in ENT was observed with higher collector dosage, which is statistically significant and is expected to lead to a considerable change in gangue recovery.

There was a visible increase in gangue recovery (and thus an increase in concentrate recovery) with increasing collector dosage in the test results. Table 6 shows that increasing ENT is significantly affected by the interaction between them. This is shown in Figure 16, which illustrates the increase

in ENT as a function of both the interaction between airflow rate and frother dosage and the interaction between airflow rate and different solid percentages.

The airflow rate has no significant effect on ENT. But the interaction between airflow rate and frother dosage, airflow rate and solid percentage has a considerable impact. Figure 17 shows, with the increase of airflow rate, ENT increased slightly. There was always a significant increase in R_w in the quartz-magnetite system compared to the increase in airflow rate.
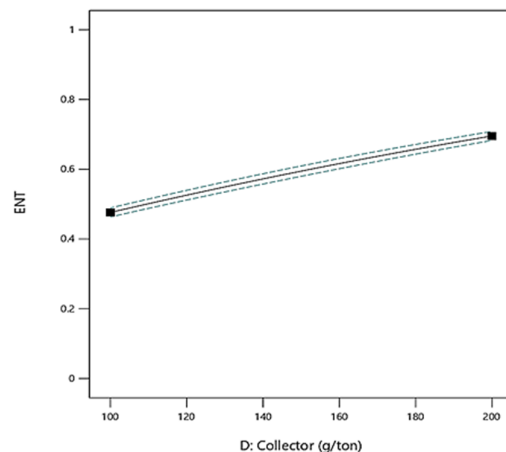

Figure 15. ENT as a function of collector agent

3.3.5. Development of ENT model based on particle mass by changing flotation operational parameters

There are many operational parameters which affect ENT. Various models about the main parameters have been suggested. Some models focus only on one or two of these parameters, while others consider multiple vital variables [39-41]. It

is worth noting that the froth structure is very complex and is affected by other factors besides particle size and density, including moisture content, airflow rate, bubble size, hydrophobic particle content, and type of reagents [29]. Therefore, it is essential to identify and experimentally quantify the effects of these variables on ENT modeling.
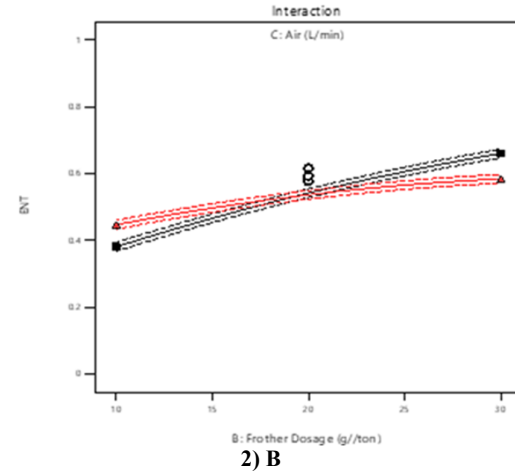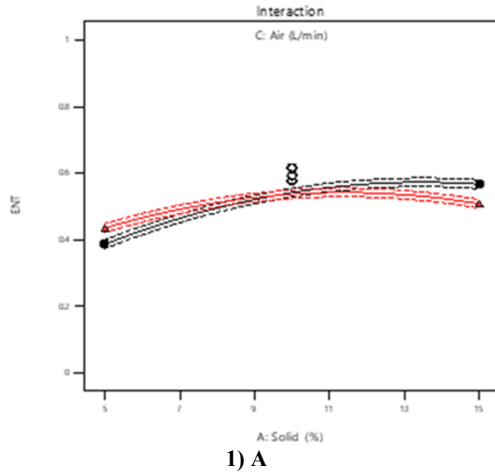
This experimental model was calculated using data from experiments. Figure 17 shows the fitting results of Savasi's ENT model. Empirical data for the one gangue mineral was used in model fitting. It can be seen that the model agrees well with the data for magnetite. The constant fitting values of ξ and δ has been found for one gangue mineral.

$\xi = 16.53\ \mu m$ and $\delta = 0.73$ for magnetite

1) A	2) B

Figure 16. a. The effect of the interaction between air flow rate and solid content, as well as b. airflow rate and frother agent on ENT.
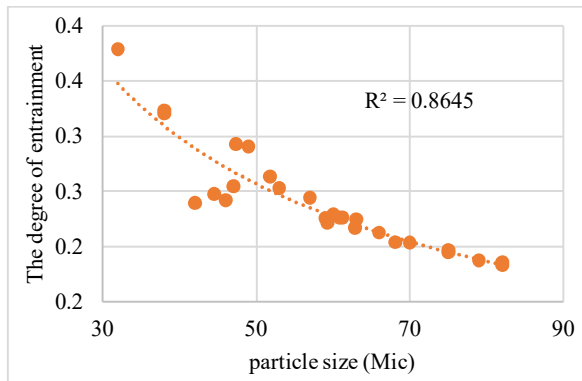

Figure 17. The result of the Savasi's ENT model to the batch experimental data for magnetite.

The ENT indicates the drainage of tracer particles to the pulp phase. The difference in the ENT value of tracer particles of different operation parameters is probably the result of the different settling rates of their particles in the water or in the froth phase, where the flow can be considered laminar. Under these situations, the sink rate of particulate matter into the fluid can be approximated using Stokes' law [35]. The weight of the solid particle in the fluid was obtained as follows:

$$G_0 = V_s.(\rho_s - \rho_w).g \qquad (11)$$

Where G_0 is the submerged weight of particles in water, V_s is the particle volume, ρ_s is the specific gravity of solid particles, ρ_w is the density of water, and g is the gravitational acceleration, which ρ_w may increase with the presence of fine suspended particles in water.

The settling velocity of the particles was the result of sufficient drag to precisely balance the immersed weight of the solid particle. Then, the settling velocity (V_{set}) will be proportional to the density difference between the tracing particles and water and the square of the particle diameter, as shown in equation 12. The quadratic relationship between settling velocity and particle size results from increasing apparent submerged weight as a function of cubic particle diameter, which must be balanced against the Stokes drag, which increases proportionally to particle size [34].

$$V_{set} = (\rho_s - \rho_w).d_1^2 \qquad (12)$$

Where the density of water is 1 g/cm^3, and the average particle size (μm) is used.

It was observed in the column flotation tests that particles with a larger size and density settle faster and experience more superb move relative to pulp phase than particles with a smaller size and density.

An empirical model was then proposed for the ENT involving $(\rho_s - \rho_w).d_1^2$, as described by

Equation 13. It is a rational function chosen because of its visual alignment with the form of the relation (see Figure 25) and corresponds to the boundary conditions of the system that was developed.

$$ENT_i = \frac{1}{1 + p((\rho_s - \rho_w).d_1^2)^q} \qquad (13)$$

Where ρ and q are constants. Equation 13 satisfies the following boundary conditions:

$$d_i \rightarrow \propto, \rho_s \rightarrow \propto \Rightarrow ENT \rightarrow 0$$

$$d_i \rightarrow \propto, \rho_s \rightarrow 0 \Rightarrow ENT \rightarrow 1$$

The model changes the particle size and the operation parameter was fixed in the past literature [33]. Figure 18 shows the results of fitting Equation 13 to the batch data reported in Table 5. The mathematical relationship fits well with the magnetite data. The relevant parameters ρ and q are:

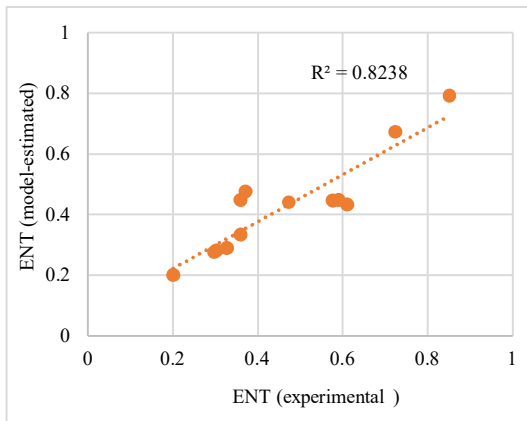$$\rho = 0.126(g\ cm^{-3}\mu m^2)^{-q} \text{ and } q=0.236.$$

Figure 18. the experimental ENT values reported in table 6 versus the outcome obtained by fitting all data using equation 13.

However, the model provides a method for accurately predicting the ENT in the column flotation feed based on operation parameters. The model also provides an estimate of the change in entrainment recovery with changes in particle size or mineral composition of the flotation column, when other flotation parameters are significantly altered.

An empirical mathematical model for ENT proposed to relate ENT to particle mass. The experimental model provides a reasonable fit to laboratory data sets, indicating that it can used to predict the ENT for minerals with different particle densities by varying different operation parameters.

6. Conclusions

A batch surface response was conducted using a mix of free quartz as a valuable mineral and a free gangue mineral, magnetite, to identify the operational parameters affecting the ENT. The obtained empirical outcome and the analysis of the conducted data allow the following conclusions:

Experimental outcomes show that the ENT varied remarkably as the flotation parameters changed, which proposes that models for the ENT that incorporate only particle size are not enough to predict R_w. A slight increase in R_w was observed with increasing solids percentage. Still, it was not statistically considerable and was not expected to result in a significant change in gangue recovery. ENT increases (0.071-0.85). This is a rather unexpected result as one would intuitively expect that increasing the frother dosage or airflow rate would result in a shorter time for draining and therefore an increase in ENT and R_w and subsequently gangue recovery.

Variations in the froth characteristics and attributes such as density of the lamellae, size of the Plateau borders and thickness are the major parameters managing the extent to which the drainage can proceed for rough entrained mass. There was a relatively strong positive correlation (0.56) between measured R_w and ENT. The collector and frother agent and the interaction between them had a statistically significant positive effect on ENT, respectively 0.54 and 0.51, which should be investigated on the effect of both parameters on ENT in the froth phase in future research.

The model of Savassi et al. (1998) for the ENT includes only the particle size and appears to fit the experimental data. An empirical mathematical model for ENT is presented to relate particle mass by changing operational parameters. The experimental model provides a reasonable fit to the column laboratory data, indicating that it can be used to predict ENT.

References

[1]. Hoang, D. H., Heitkam, S., Kupka, N., Hassanzadeh, A., Peuker, U. A., & Rudolph, M. (2019). Froth properties and entrainment in lab-scale flotation: A case of carbonaceous sedimentary phosphate ore. *Chemical Engineering Research and Design*, *142*, 100-110.

[2]. Norori-McCormac, A., Brito-Parada, P. R., Hadler, K., Cole, K., & Cilliers, J. J. (2017). The effect of particle size distribution on froth stability in

flotation. *Separation and Purification Technology*, *184*, 240-247.

[3]. Bhambhani, T., Farinato, R., Nagaraj, D. R., & Somasundaran, P. (2023). Effect of platy gangue minerals in sulfide flotation: Part I-transport rates. *Minerals Engineering*, *201*, 108185.

[4]. Mathe, Z. T., Harris, M. C., O'Connor, C. T., & Franzidis, J. P. (1998). Review of froth modelling in steady state flotation systems. *Minerals Engineering*, *11*(5), 397-421.

[5]. Mathe, Z. T., Harris, M. C., & O'Connor, C. T. (2000). A review of methods to model the froth phase in non-steady state flotation systems. *Minerals Engineering*, *13*(2), 127-140.

[6]. Wang, D., & Liu, Q. (2021). Hydrodynamics of froth flotation and its effects on fine and ultrafine mineral particle flotation: A literature review. *Minerals Engineering*, *173*, 107220.

[7]. Azizi, A. (2017). A study on the modified flotation parameters and selectivity index in copper flotation. *Particulate science and technology*, *35*(1), 38-44.

[8]. Vieira, A. M., & Peres, A. E. (2007). The effect of amine type, pH, and size range in the flotation of quartz. *Minerals Engineering*, *20*(10), 1008-1013.

[9]. Vera, M. A., Mathe, Z. T., Franzidis, J. P., Harris, M. C., Manlapig, E. V., & O'Connor, C. T. (2002). The modelling of froth zone recovery in batch and continuously operated laboratory flotation cells. *International Journal of Mineral Processing*, *64*(2-3), 135-151.

[10]. Nakhaei, F., Mosavi, M. R., Sam, A., & Vaghei, Y. (2012). Recovery and grade accurate prediction of pilot plant flotation column concentrate: Neural network and statistical techniques. *International Journal of Mineral Processing*, *110*, 140-154.

[11]. Finch, J. A., & Dobby, G. S. (1990). Column flotation. *Flotation Science and Engineering*, 291-329.

[12]. Xu, M., Finch, J. A., & Uribe-Salas, A. (1991). Maximum gas and bubble surface rates in flotation columns. *International journal of mineral processing*, *32*(3-4), 233-250.

[13]. Reddy, P. S. R., Kumar, S. G., Bhattacharyya, K. K., Sastri, S. R. S., & Narasimhan, K. S. (1988). Flotation column for fine coal beneficiation. *International Journal of Mineral Processing*, *24*(1-2), 161-172.

[14]. Dey, S., Pani, S., Singh, R., & Paul, G. M. (2015). Response of process parameters for processing of iron ore slime using column flotation. *International Journal of Mineral Processing*, *140*, 58-65.

[15]. YANG, C. H., XU, C. H., Mu, X. M., & ZHOU, K. J. (2009). Bubble size estimation using interfacial morphological information for mineral flotation process

monitoring. *Transactions of Nonferrous Metals Society of China*, *19*(3), 694-699.

[16]. Bouaifi, M., Hebrard, G., Bastoul, D., & Roustan, M. (2001). A comparative study of gas hold-up, bubble size, interfacial area and mass transfer coefficients in stirred gas–liquid reactors and bubble columns. *Chemical engineering and processing: Process intensification*, *40*(2), 97-111.

[17]. Shean, B. J., & Cilliers, J. J. (2011). A review of froth flotation control. *International Journal of Mineral Processing*, *100*(3-4), 57-71.

[18]. Neethling, S. J., & Cilliers, J. J. (2002). The entrainment of gangue into a flotation froth. *International Journal of Mineral Processing*, *64*(2-3), 123-134.

[19]. Engelbrecht, J. A., & ET, W. (1975). The effects of froth height, aeration rate, and gas precipitation on flotation.

[20]. Jowett, A. (1966). FLOTATION KINETICS.. GANGUE MINERAL CONTAMINATION OF FROTH. *Brit Chem Eng*, *11*(5), 330-333.

[21]. Laplante, A. R., Kaya, M., & Smith, H. W. (1989). The effect of froth on flotation kinetics-A mass transfer approach. *Mineral Procesing and Extractive Metallurgy Review*, *5*(1-4), 147-168.

[22]. Akdemir, Ü., & Sönmez, İ. (2003). Investigation of coal and ash recovery and entrainment in flotation. *Fuel Processing Technology*, *82*(1), 1-9.

[23]. Wang, L., Peng, Y., & Runge, K. (2016). Entrainment in froth flotation: The degree of entrainment and its contributing factors. *Powder Technology*, *288*, 202-211.

[24]. Cilek, E. C. (2009). The effect of hydrodynamic conditions on true flotation and entrainment in flotation of a complex sulphide ore. *International Journal of Mineral Processing*, *90*(1-4), 35-44.

[25]. Wang, C., Sun, C., & Liu, Q. (2021). Entrainment of gangue minerals in froth flotation: mechanisms, models, controlling factors, and abatement techniques—a review. *Mining, Metallurgy & Exploration*, *38*(2), 673-692.

[26]. Quintanilla, P., Neethling, S. J., & Brito-Parada, P. R. (2021). Modelling for froth flotation control: A review. *Minerals Engineering*, *162*, 106718.

[27]. Anzoom, S. J., Bournival, G., & Ata, S. (2024). Coarse particle flotation: A review. *Minerals Engineering*, *206*, 108499.

[28]. Yang, B., Yin, W., Zhu, Z., Wang, D., Han, H., Fu, Y., ... & Yao, J. (2019). A new model for the degree of entrainment in froth flotation based on mineral particle characteristics. *Powder technology*, *354*, 358-368.

[29]. Zheng, X., Johnson, N. W., & Franzidis, J. P. (2006). Modelling of entrainment in industrial flotation

cells: Water recovery and degree of entrainment. *Minerals Engineering*, *19*(11), 1191-1203.

[30]. *Wang, L., Peng, Y. and Runge, K., 2016. Entrainment in froth flotation: The degree of entrainment and its contributing factors. Powder Technology, 288, pp.202-211.*

[31]. Wang, L., Runge, K., Peng, Y., & Vos, C. (2016). An empirical model for the degree of entrainment in froth flotation based on particle size and density. *Minerals Engineering*, *98*, 187-193.

[32]. Vining, G. (2010). Technical advice: residual plots to check assumptions. *Quality Engineering*, *23*(1), 105-110.

[33]. Melo, F., & Laskowski, J. S. (2007). Effect of frothers and solid particles on the rate of water transfer to froth. *International Journal of Mineral Processing*, *84*(1-4), 33-40.

[34]. Wiese, J., & Harris, P. (2012). The effect of frother type and dosage on flotation performance in the presence of high depressant concentrations. *Minerals Engineering*, *36*, 204-210.

[35]. Lima, N. P., de Souza Pinto, T. C., Tavares, A. C., & Sweet, J. (2016). The entrainment effect on the performance of iron ore reverse flotation. *Minerals Engineering*, *96*, 53-58.

[36]. Wang, L., Xing, Y., & Wang, J. (2020). Mechanism of the combined effects of air rate and froth depth on entrainment factor in copper flotation. *Physicochemical Problems of Mineral Processing*, *56*.

[37]. Ata, S. (2012). Phenomena in the froth phase of flotation—A review. *International Journal of Mineral Processing*, *102*, 1-12.

[38]. Popli, K., Afacan, A., Liu, Q., & Prasad, V. (2018). Real-time monitoring of entrainment using fundamental models and froth images. *Minerals Engineering*, *124*, 44-62.

[39]. Neethling, S. J., & Cilliers, J. J. (2002). The entrainment of gangue into a flotation froth. *International Journal of Mineral Processing*, *64*(2-3), 123-134.

[40]. Yang, B., Yin, W., Zhu, Z., Wang, D., Han, H., Fu, Y., ... & Yao, J. (2019). A new model for the degree of entrainment in froth flotation based on mineral particle characteristics. *Powder technology*, *354*, 358-368.

[41]. Amelunxen, P., LaDouceur, R., Amelunxen, R., & Young, C. (2018). A phenomenological model of entrainment and froth recovery for interpreting laboratory flotation kinetics tests. *Minerals Engineering*, *125*, 60-65.

[42]. Kursun, H. (2017). The influence of frother types and concentrations on fine particles' entrainment using column flotation. *Separation Science and Technology*, *52*(4), 722-731.

مدلی تجربی برای تعیین درجه دنباله‌روی در فلوتاسیون ستونی بر اساس پارامترهای عملیاتی

رضا ذوالفقاری و محمد کارآموزیان*

دانشکده مهندسی معدن، نفت و ژئوفیزیک، دانشگاه صنعتی شاهرود، شاهرود، ایران

٭ نویسنده مسئول مکاتبات: m.karamoozian@shahroodut.ac.ir

چکیده:

در فلوتاسیون، دنباله‌روی (ENT) بر بازیابی کنسانتره تأثیر می‌گذارد و مدل دنباله‌روی اغلب تنها تابعی از اندازه ذرات در مدل‌ها است. برخی از تحقیقات نشان می‌دهد که متغیرهای دیگر نیز ممکن است به طور قابل توجهی بر ENT تأثیر بگذارند. در این مطالعه، سری از آزمایش‌های فلوتاسیون با استفاده از مخلوط کوارتز خالص به عنوان کانی ارزشمند و نمونه مگنتیت خالص به عنوان کانی گانگ برای بررسی اثرات سایر متغیرها مانند درصد جامد، دبی هوا، غلظت کف‌ساز و کلکتور بر روی درجه دنباله‌روی انجام شدند. نتایج نشان داد که درجه دنباله‌روی از ۰/۰۷۱ تا ۰/۸۵۱ متغیر است، در حالی که بازیابی دنباله‌روی بین ۰/۰۰۶ تا ۰/۲۳ بود که این تفاوت از نظر آماری معنادار است. درجه دنباله‌روی تحت تأثیر (۱) غلظت کلکتور، (۲) غلظت کف‌ساز، (۳) محتوای جامد، (۴) برهمکنش بین دبی هوا و درصد جامد و (۵) تعامل بین دبی هوا و غلظت کف‌ساز. یک مدل آماری تجربی بر اساس پارامترهای عملیاتی ارائه شد. از آنجایی که مدل‌های فعلی برای درجه دنباله‌روی فقط اندازه ذرات را در بر می‌گیرند، پیش‌بینی بازیابی گانگ در کاربردهای صنعتی با ثابت نگه داشتن شرایط عملیاتی کافی نیست. این مدل جدید می تواند درجه دنباله‌روی را بر اساس پارامترهای عملیاتی مختلف پیش بینی کند. مدل توسعه یافته بر اساس جرم ذرات با تغییر پارامترهای عملیاتی ارائه شده است.

کلمات کلیدی: فلوتاسیون ستونی، درجه دنباله‌روی، بازیابی آب، بازیابی کنسانتره، مدل تجربی.